

# Prediction of Elastic Properties of Multi-Layered Epoxy Composites Reinforced with Pineapple Leaf Fiber and Grewia Optiva Using Classical Laminate Plate Theory

Mayank Bharadvaj<sup>1</sup>, Jitendra Yadav<sup>2</sup>, Brijesh Gangil<sup>3</sup>

<sup>1</sup>Research Scholar, Department of Mechanical Engineering, SOAE, UPES, Dehradun, India

<sup>2</sup>Professor, Department of Mechanical Engineering, SOAE, UPES, Dehradun, India

<sup>3</sup>Professor, Department of Mechanical Engineering, H.N.B. Garhwal University, 246174, India

Corresponding Author: [Mayank Bharadvaj](#)

**Abstract:** Natural fiber composites are increasingly adopted due to sustainability and lightweight requirements. This work predicts the elastic constants of epoxy-based hybrid laminates reinforced with Pineapple Leaf Fiber (PALF) and Grewia Optiva using Classical Laminate Plate Theory (CLPT). Three stacking sequences— $[0/\pm 45/90]$  (A<sub>1</sub>),  $[0/(45)_2/-30]$  (A<sub>2</sub>), and  $[0/45/90/30]$  (A<sub>3</sub>)—were modeled with PALF content varying from 10 wt.% to 20 wt.% and Grewia Optiva fixed at 20 wt.%. Increasing PALF content enhanced stiffness, with the highest longitudinal modulus (37.32 GPa) obtained for A<sub>3</sub>. A<sub>1</sub> exhibited maximum shear modulus (14.56 GPa), whereas A<sub>2</sub> demonstrated the highest Poisson's ratio (0.31). The results indicate that stacking sequence significantly governs anisotropic behavior, with A<sub>3</sub> achieving the most balanced stiffness profile. The study demonstrates that CLPT provides a computationally efficient tool for hybrid natural fiber laminate design. Future work will experimentally validate the predictions and include hygro-thermal considerations.

**Keywords:** Natural fiber composites, Pineapple Leaf Fiber, Grewia Optiva, Classical Laminate Plate Theory, stacking sequence, elastic properties.

## Nomenclature

Details of Symbols		Dimensionless Parameters	
Symbol	Definition (Unit)	Parameter	Definition
E	Young's Modulus (GPa)	$\mu_{xy}$	Poisson's ratio (major)
G	Shear Modulus (GPa)	$\lambda$	Load factor / Stacking efficiency
V	Volume fraction		
t	Lamina thickness (mm)		
z	Distance from laminate mid-plane (mm)		
Q	Reduced stiffness matrix		
T	Transformation matrix		
A	Extensional stiffness matrix		

Greek Symbols	Definition (Unit)
$\nu$ (nu)	Poisson's ratio (–)
$\delta$	Laminate deformation or elongation (mm)
$\sigma$	Stress (MPa)
$\tau$	Shear stress (MPa)
$\epsilon$	Strain (–)
Abbreviations	Definition
PALF	Pineapple Leaf Fiber
CLPT	Classical Laminate Plate Theory
FEM	Finite Element Method
RVE	Representative Volume Element
wt. %	Weight percent

$A_1, A_2, A_3$	Laminate stacking sequence designations
$E_{xx}$	Longitudinal modulus
$E_{yy}$	Transverse modulus
$G_{xy}$	In-plane shear modulus

## Introduction

In recent years, sustainability has emerged as a critical driver in the development of engineering materials, particularly in industries such as automotive, aerospace, and civil infrastructure<sup>1</sup>. The need for lightweight, eco-friendly, and cost-effective materials has intensified as global regulations tighten and industries move towards reducing carbon footprints<sup>2</sup>. Conventional petroleum-based composites, though mechanically robust, present significant environmental concerns due to their non-biodegradability, high energy demand in production, and disposal challenges<sup>3, 4, 5</sup>. This shift in priorities has accelerated the adoption of bio-based composites, which integrate renewable resources into material design, aligning with international initiatives for climate change mitigation and circular economy practices<sup>6,7</sup>. Natural fiber-reinforced composites (NFRPs) have been extensively explored owing to their advantages such as low density, biodegradability, cost-effectiveness, and reasonable mechanical strength<sup>8,9</sup>. Fibers like flax, jute, hemp, and sisal have demonstrated potential in delivering strength-to-weight ratios comparable to synthetic reinforcements such as glass fibers, while offering reduced environmental impact<sup>10,11</sup>. Applications of these composites span automotive interiors, building panels, sports equipment, and packaging<sup>12,13</sup>. However, the full-scale adoption of NFRPs remains constrained by variability in fiber properties, moisture sensitivity, and challenges in achieving consistent mechanical performance<sup>14,15</sup>. Continuous research is therefore required to optimize their design and expand their application scope<sup>16</sup>.

Literature reports highlight significant progress in hybrid composites, where combinations of different natural fibers are used to balance mechanical and functional properties<sup>17,18</sup>. For instance, Venkateshwaran et al. compared banana-sisal hybrid composites, showing improvements in tensile strength through fiber synergy<sup>19</sup>. Jogur Ganesh et al. applied higher-order finite element methods (FEM) to model jute-flax composites, while Wang and Huang employed laminate theory to predict biaxial stresses in fiber laminates<sup>20</sup>. Recent studies have also demonstrated that fiber orientation and stacking sequence strongly

influence stiffness, shear response, and anisotropy of composite laminates<sup>21,22</sup>. These findings underline the importance of modeling techniques for accurate prediction of mechanical behavior prior to experimental validation.

More recent research (last 3–4 years) has shifted toward lightweight hybrid laminates reinforced with unconventional natural fibers<sup>23,24</sup>. Studies on fibers such as pineapple leaf fiber (PALF) and Grewia Optiva report promising stiffness-to-weight characteristics. PALF, with a high Young's modulus, provides substantial axial stiffness, while Grewia Optiva contributes low density and reasonable shear strength<sup>25,26</sup>. Although both fibers have been individually explored, their hybrid combination remains largely under-investigated. Furthermore, limited work has focused on systematically correlating fiber content, stacking sequence, and elastic constants through computational models<sup>27,28,29</sup>. The reliance on FEM for such analysis, though accurate, remains computationally intensive, limiting its use for rapid design evaluation<sup>30,31</sup>.

**The literature reveals three major gaps:** (i) limited systematic studies on hybrid PALF–Grewia Optiva composites<sup>32,33</sup> (ii) insufficient exploration of stacking sequence effects on elastic constants<sup>34,35</sup> and (iii) lack of fast, computationally efficient predictive models as alternatives to FEM<sup>36,37</sup>. Addressing these gaps is essential to enable practical use of bio-composites in industries where design efficiency, reproducibility, and sustainability are critical.

The present study aims to develop a quasi-mathematical model, based on Classical Laminate Plate Theory (CLPT), to predict the elastic properties of multi-layered epoxy composites reinforced with PALF and Grewia Optiva fibers. Specifically, the objectives are:

- To analyze the effect of stacking sequence on longitudinal modulus, transverse modulus, shear modulus, and Poisson's ratio.
- To examine the influence of PALF content (10–20 wt.%) while keeping Grewia Optiva constant at 20 wt.%.
- To validate CLPT-based predictions as a computationally efficient alternative to FEM for hybrid bio-composite design.

The novelty of this work lies in integrating underutilized natural fibers into a hybrid laminate architecture and demonstrating a modeling approach that balances accuracy with computational efficiency. The outcomes provide insights for optimizing eco-friendly

laminates, particularly for structural and automotive applications. The remainder of the paper is structured as follows: Section 2 describes the theoretical framework based on CLPT, Section 3 presents the methodology, Section 4 discusses the results and their implications, and Section 5 concludes with key findings and future research directions.

## 2. Classical laminate plate theory

By knowing Young's modulus for fiber and matrix separately the Young's modulus for resulting lamina can be calculated using rule of mixture. In the first step, the rule of mixture is used for obtaining the elastic properties of single lamina followed by reduced stiffness matrix  $[Q]$ <sup>38</sup>. The following formulas are used for obtaining effective elastic properties for single lamina.

Young Modulus of composite in the direction of fiber is presented by equation 1.

$$E_{11} = E_f * F + E_m * M + E_{PF} * VPF \quad (1)$$

Young Modulus perpendicular to the direction of Fiber is presented in equation 2.

$$E_{22} = (E_f * E_m * E_{PF}) / (E_f * E_{PF} * M + E_m * E_{PF} * F + E_f * E_m * VPF) \quad (2)$$

Shear modulus is presented by equation 3.

$$G_{12} = (G_M * G_f * G_{PF}) / (M * G_f * G_{PF} + G_M * G_f * VPF + G_M * F * G_{PF}) \quad (3)$$

Poisson ratio is presented by equation 4.

$$\mu_{12} = \mu_{21} = F * \mu_f + VPF * \mu_{PF} + M * \mu_m \quad (4)$$

Where, E is used for Young Modulus, G for shear Modulus, f for fiber, m for matrix, PF for PALF, VPF, M and F for volumetric fraction of PALF, matrix and fiber respectively. A reduced stiffness matrix  $[Q]$  is obtained from the above results as shown by equation 5.

$$[Q] = \begin{bmatrix} E_{11}/(1 - \mu_{12}\mu_{21}) & E_{22}\mu_{12}/(1 - \mu_{12}\mu_{21}) & 0 \\ E_{22}\mu_{12}/(1 - \mu_{12}\mu_{21}) & E_{22}/(1 - \mu_{12}\mu_{21}) & 0 \\ 0 & 0 & G_{12} \end{bmatrix} \quad (5)$$

For different degrees of rotation, transformation matrix  $[T]$  was used as follows in equation 6.

$$[T] = \begin{bmatrix} \cos^2[\theta] & \sin^2[\theta] & 2\cos[\theta]\sin[\theta] \\ \sin^2[\theta] & \cos^2[\theta] & -2\cos[\theta]\sin[\theta] \\ -\cos[\theta]\sin[\theta] & \cos[\theta]\sin[\theta] & \cos^2[\theta] - \sin^2[\theta] \end{bmatrix} \quad (6)$$

Reuter Matrix  $[R]$  is presented by equation 7

$$[R] = \begin{bmatrix} 1 & 0 & 0 \\ 0 & 1 & 0 \\ 0 & 0 & 2 \end{bmatrix} \quad (7)$$

After finding all these values, Transformed reduced stiffness matrix  $[\bar{Q}]$  was obtained as shown in equation 8

$$[\bar{Q}] = \text{Inverse}[T] \cdot [Q] \cdot [R] \cdot [T] \cdot \text{Inverse}[R] \quad (8)$$

Next step is to obtain extensional stiffness matrix  $[A]$ , which is obtained by given formula in equation 9.

$$A_{ij} = \sum_{k=1}^n [\bar{Q}_{ij}] (z_k - z_{k-1}) = \sum_{k=1}^n [\bar{Q}_{ij}] (t_k) \quad (9)$$

Where,  $\bar{Q}_{ij}$  stands for the reduced stiffness matrix of alignment,  $z$  stands for the distance of lamina from centre, and  $t_k$  stands for thickness of lamina is shown in figure 1. It is depicted that the stacking sequences of the three composite laminates evaluated:  $A_1$ ,  $A_2$ , and  $A_3$ . The configurations differ in ply orientation and number of layers, which directly influence the predicted elastic constants. The  $A_1$  laminate uses a balanced symmetric layup of  $[0/\pm 45/90]$ , while  $A_2$  introduces an asymmetric design with repeated  $45^\circ$  plies and a  $-30^\circ$  ply, and  $A_3$  combines four distinct orientations:  $0^\circ$ ,  $45^\circ$ ,  $90^\circ$ , and  $30^\circ$ . These variations enable the study to explore how ply orientation affects longitudinal modulus, transverse modulus, shear modulus, and Poisson's ratio in multi-layered bio-composites. In the study the thickness of lamina is 10mm. The above equation can further be simplified for  $A_1$  laminate as shown by equation 10.

$$A = \bar{Q}_0 t_1 + \bar{Q}_{45} t_2 + \bar{Q}_{-45} t_3 + \bar{Q}_{90} t_4 \quad (10)$$

Similarly, extensional stiffness matrix  $[A]$  is obtained for another combination. In the next step  $[A]^{-1}$  is obtained, which provides the values of different elastic constants as given below: -

$$E_{xx} = 1/t \cdot a_{11}$$

$$E_{yy} = 1/t \cdot a_{22}$$

$$G_{xy} = 1/t \cdot a_{66}$$

$$\mu_{xy} = -a_{12}/a_{11}$$

The elastic constants for all the combinations are obtained through the above steps.

### 3. Methodology

In this study, three laminates of stacking sequences  $[0/\pm 45/90]$  ( $A_1$ ),  $[0/(45)_2/-30]$  ( $A_2$ ) and  $[0/45/90/30]$  ( $A_3$ ) were used. The materials taken for the study were epoxy LY 556, PALF, and Grewia Optiva. For research purposed Grewia Optiva was fixed at 20 wt. %, and PALF was

varied between 10 to 15 wt. % in steps of 5, the remaining portion was epoxy LY 556.

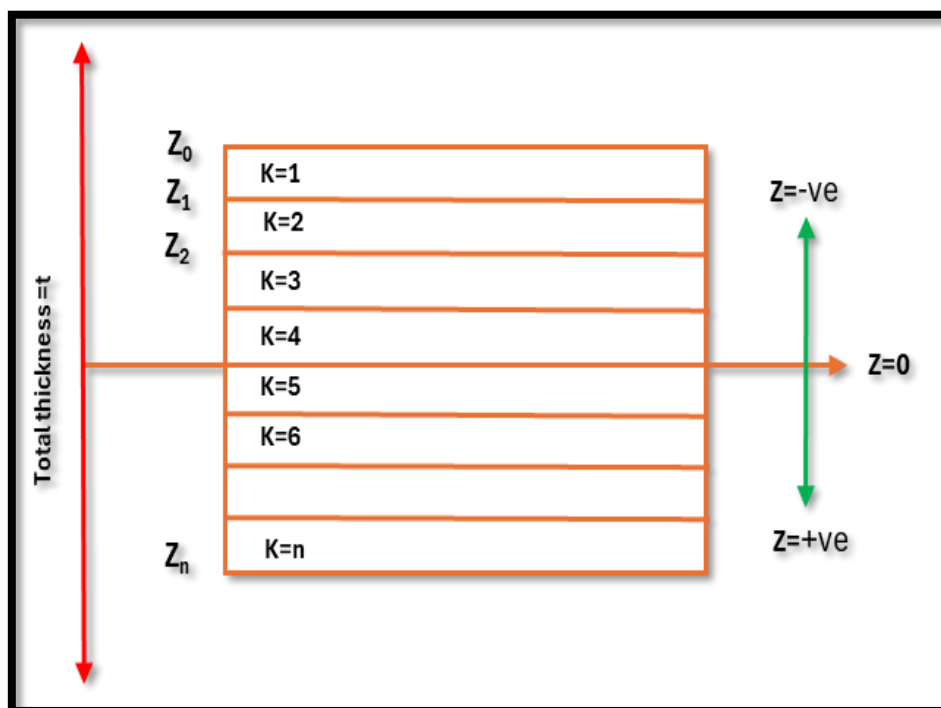


**Figure 1: Representation of stacking sequence**

The properties required for the modeling purpose and compositions are mentioned in Table 1 and Table 2. Table 1 presents the fundamental material properties required for the modelling: density, Young's modulus, shear modulus, and Poisson's ratio for the epoxy matrix (LY 556), Grewia Optiva fiber, and Pineapple Leaf Fiber (PALF). Among these, PALF exhibits the highest stiffness, with a Young's modulus of 34.5 GPa, which is four times that of Grewia Optiva (8.6 GPa) and about ten times higher than that of the epoxy matrix (3.47 GPa). This notable difference highlights PALF's significant contribution to enhancing the composite's overall stiffness, while Grewia Optiva, though less stiff, brings other benefits such as lower density ( $0.45 \text{ g/cm}^3$ ), which aids in weight reduction. Table 2 summarizes the composition designations used for modelling. Grewia Optiva content is held constant at 20 wt.% across all combinations, while PALF content is varied incrementally from 10 wt.% (PALF 1) to 20 wt.% (PALF 2). This variation results in a corresponding decrease in epoxy content from 70 wt.% to 60 wt.%, allowing the study to examine how increasing PALF fraction affects the mechanical properties of the laminates.

**Table 1: Mechanical properties of constituent materials used in modeling (Epoxy LY 556, Grewia Optiva fiber, and PALF)**

S.N.	Materials	Density (g/cm <sup>3</sup> )	Young Modulus (GPa)	Shear Modulus (GPa)	Poisson Ratio
1	Epoxy LY 556	1.14	3.47	2.10	0.30
2	Grewia Optiva	0.45	8.6	3.25	0.32
3	Pineapple	1.52	34.5	11.5	0.2

**Table 2: Composite formulations with varying PALF content and constant Grewia Optiva content**

S.N.	Designation	Composition		
		Epoxy LY 556 (wt. %)	PALF (wt. %)	GrewiaOptiva (wt. %)
1	PALF 1	70	10	20
2	PALF 1.5	65	15	20
3	PALF 2	60	20	20

The designation of stacking is represented in Table 3, which outlines the stacking sequence designations for the three laminate configurations studied:  $[0/\pm 45/90]$  (A<sub>1</sub>),  $[0/(45)_2/-30]$  (A<sub>2</sub>), and  $[0/45/90/30]$  (A<sub>3</sub>). These sequences differ in ply orientation and symmetry, directly influencing stiffness and anisotropy. For instance, A<sub>1</sub> has a balanced and symmetric layup, while A<sub>2</sub> introduces asymmetry and repeated 45° plies, and A<sub>3</sub> combines multiple angles to potentially optimize in-plane properties.

**Table 3: Stacking sequence designations of composite laminates**

S.N.	Combination	Designation
1	$0/\pm 45/90$	A <sub>1</sub>
2	$0/(45)_2/30$	A <sub>2</sub>
3	$0/45/90/30$	A <sub>3</sub>

These tables provide a structured basis for the mathematical modelling; highlighting how differences in fiber content and layup design can significantly affect predicted elastic

properties of the composite laminates.

Classical laminate plate theory was used to determine in-plane elastic constants in different stacking. Mathematical modeling was completed in Wolfram Mathematics.

## 4. Result and Discussion

### 4.1 Longitudinal Modulus

Figure 2 illustrates how the longitudinal modulus ( $E_{xx}$ ) varies with increasing PALF content across the three stacking sequences. The results clearly show that  $E_{xx}$  increases as PALF volume fraction rises from 10 wt.% to 20 wt.%, reflecting the higher stiffness contribution of PALF. Among the laminates,  $A_3$  achieves the highest longitudinal modulus for all compositions, reaching 37.32 GPa at the highest PALF content, whereas  $A_2$  consistently exhibits the lowest  $E_{xx}$  values. These trends confirm that laminate architecture, specifically the distribution and orientation of plies, plays a decisive role in enhancing axial stiffness, alongside the effect of fiber loading. It appears that improved longitudinal modulus is the result of dense stacking and efficient stress transfer.

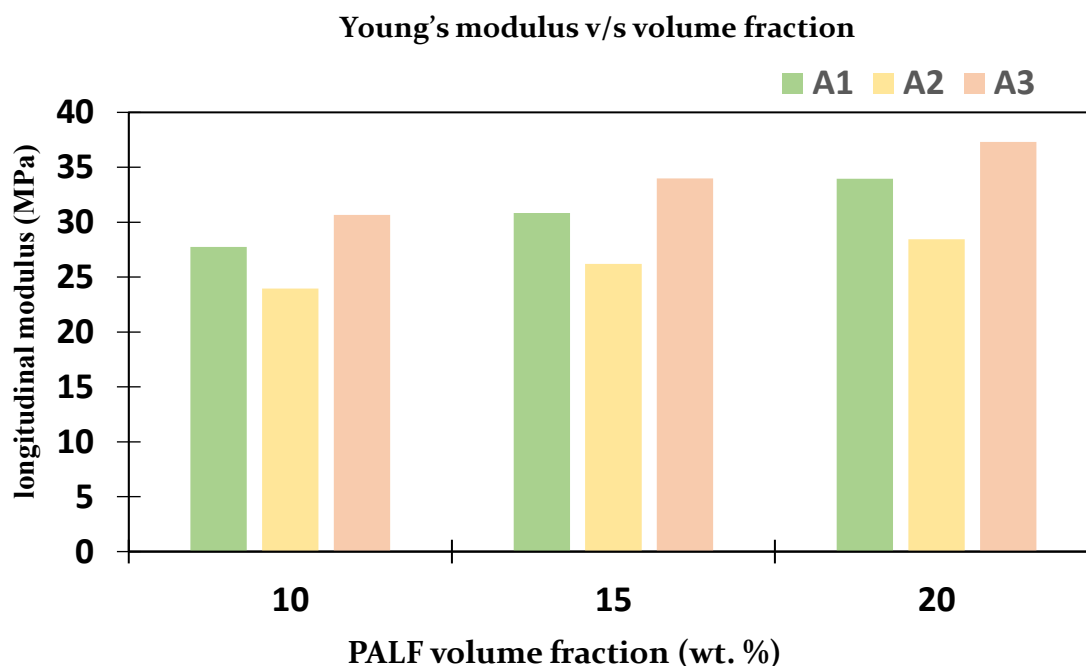


**Figure 2: Variation of longitudinal modules ( $E_{xx}$ ) with increasing PALF content across different stacking sequences**

### 4.2 Transverse Modulus

The value of transverse modulus increases with increase in fiber volume fraction of PALF (Figure 3). It is worth noticing that the value of transverse modulus is equal to longitudinal

modulus for A<sub>1</sub> type of stacking, but the transverse modulus value for A<sub>2</sub> and A<sub>3</sub> type, stacking drops as the fiber volume fraction increases. In all the stacking sequences A<sub>2</sub> type of sequence has the lowest value of transverse modulus followed by A<sub>3</sub>. The layup direction impacts the results due to distribution of strength. The outcome produced by this mathematical model is comparable to that of FEM tool, which shows that the shear modulus value improves as the fiber volume fraction increases.

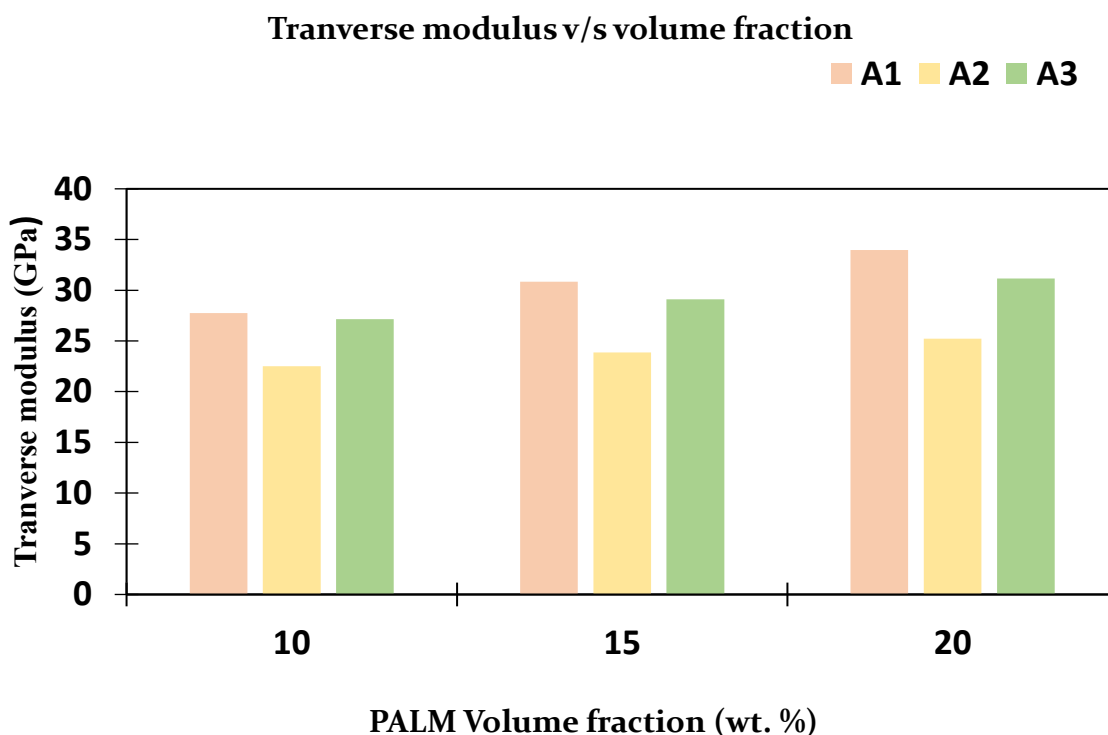


**Figure 3: Variation of transverse modulus ( $E_{yy}$ ) with PALF content for different stacking sequences**

### 4.3 Shear Modulus

The value of shear modulus predicted by mathematical model is presented in figure 4. The graph shows that the value of shear modulus depends on fiber volume fraction. The shear modulus value is found to be maximum for A<sub>1</sub> stacking followed by A<sub>3</sub> and A<sub>2</sub>, for all volume fractions. Y. S. Munde et al.<sup>48)</sup> has reported the same relation of shear modulus with fiber volume fraction.

### 4.4 Poisson Ratio

As illustrated in Figure 5, Poisson's ratio is highest for the A<sub>2</sub> laminate across all compositions, reaching around 0.31 at 20 wt.% PALF. This reflects A<sub>2</sub>'s greater transverse compliance due to

ply orientation. In contrast, A1 and A3 have lower and relatively stable  $\mu_{xy}$  values.

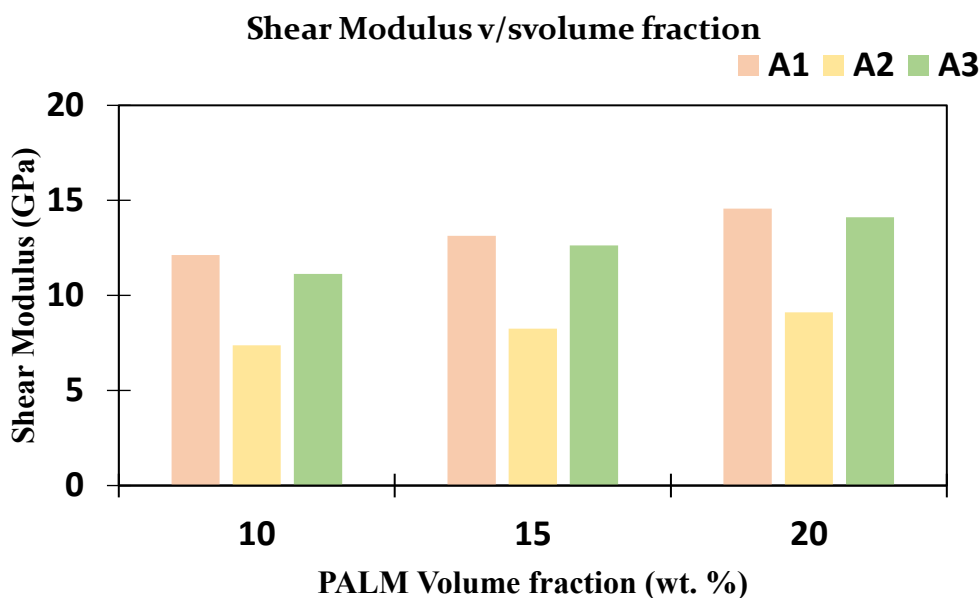


**Figure 4:** Predicted shear modulus ( $G_{xy}$ ) as a function of PALF content across stacking sequences

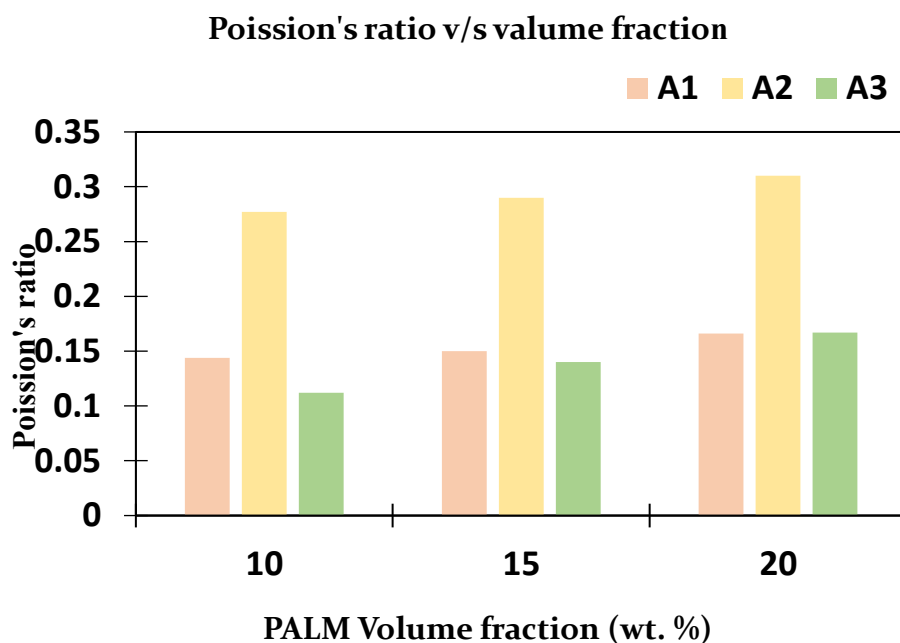


**Figure 5:** Poisson's ratio ( $\mu_{xy}$ ) variation with PALF content for different stacking sequences.

The detailed predicted elastic constants for each stacking sequence and PALF content are summarized in Table 4.

**Table 4. Predicted elastic properties ( $E_{xx}$ ,  $E_{yy}$ ,  $G_{xy}$ ,  $\mu_{xy}$ ) of composite laminates for different stacking sequences and PALM content**

Composition (PALF wt.%)	Type	$E_{xx}$ (GPa)	$E_{yy}$ (GPa)	$G_{xy}$ (GPa)	$\mu_{xy}$
PALF 1(10 wt.% PALF, 20 wt.% Grewia Optiva)	A1	27.76	27.76	12.13	0.144
	A2	23.97	22.50	7.37	0.277
	A3	30.65	27.14	11.14	0.112
PALF 1.5(15 wt.% PALF, 20 wt.% Grewia Optiva)	A1	30.83	30.83	13.13	0.150
	A2	26.19	23.86	8.25	0.290
	A3	33.98	29.12	12.63	0.140
PALF 2(20 wt.% PALF, 20 wt.% Grewia Optiva)	A1	33.96	33.96	14.56	0.166
	A2	28.46	25.22	9.11	0.310
	A3	37.32	31.17	14.12	0.167

It summarizes the predicted elastic properties of the composite laminates for three stacking sequences (A1, A2, A3) at increasing PALF content (10 wt.%, 15 wt.%, and 20 wt.%), keeping Grewia Optiva fixed at 20 wt.%.

**The results reveal clear trends:**

- Longitudinal modulus ( $E_{xx}$ ) consistently increases as PALF content rises, with A3 always achieving the highest  $E_{xx}$ , peaking at 37.32 GPa for PALF 2.
- Transverse modulus ( $E_{yy}$ ) follows a similar trend, also higher for A1 and A3, while A2 consistently shows lower values due to its stacking configuration.
- Shear modulus ( $G_{xy}$ ) increases with PALF content, with A1 typically slightly higher than A3; A2 remains lowest across all compositions.
- Poisson's ratio ( $\mu_{xy}$ ) is notably higher for A2 in all cases (e.g., 0.310 for PALF 2), reflecting the greater transverse compliance caused by its ply orientation, whereas A1 and A3 maintain lower and closer values.

Beyond the observed trends, clear correlations emerge between stacking sequence, PALF content, and elastic properties:

- The increase in longitudinal modulus ( $E_{xx}$ ) with PALF content is nearly linear for all stacking sequences, but the slope is highest for A<sub>3</sub> and lowest for A<sub>2</sub>. This suggests that A<sub>3</sub>'s diverse ply orientations (0°, 45°, 90°, 30°) facilitate more effective stress transfer along the fiber direction.
- For transverse modulus ( $E_{yy}$ ), A<sub>1</sub> consistently outperforms A<sub>2</sub> and A<sub>3</sub>, which can be attributed to its balanced and symmetric layup ([0/±45/90]). This configuration distributes loads more uniformly across the laminate, resulting in greater transverse stiffness.
- The behaviour of **shear modulus** ( $G_{xy}$ ) aligns closely with that of  $E_{xx}$ , indicating a positive correlation between axial stiffness and shear rigidity. Laminates with higher  $E_{xx}$  tend to exhibit higher  $G_{xy}$ , underscoring the influence of PALF's higher shear modulus (11.5 GPa) on overall composite shear performance.
- Interestingly, **Poisson's ratio** ( $\mu_{xy}$ ) shows an inverse correlation with stiffness. The A<sub>2</sub> laminate, which has the lowest  $E_{xx}$  and  $G_{xy}$ , exhibits the highest  $\mu_{xy}$ . This can be interpreted as greater transverse deformation per unit axial load, likely due to the asymmetric ply arrangement and concentration of ±45° layers in A<sub>2</sub>.

These correlations emphasize that while increasing PALF content enhances stiffness in all directions, the stacking sequence governs the degree and efficiency of this enhancement. The A<sub>3</sub> laminate offers the best balance between axial and transverse stiffness, whereas A<sub>2</sub>, despite having higher Poisson's ratio, underperforms in stiffness parameters due to its asymmetric design.

The mathematical model predictions align with known trends reported in earlier studies (e.g., Venkateshwaran et al. and Munde et al.), supporting the validity of the quasi-numerical modelling approach. The model's ability to capture differences between stacking sequences demonstrates its potential usefulness for optimizing laminate design a priori, before costly experiments.

These findings highlight the importance of tailoring both fiber content and stacking architecture when designing bio-based composite laminates, as the interplay between material properties and ply orientation significantly affects mechanical performance.

## 5. Conclusion

The present study developed a quasi-mathematical framework using Classical Laminate Plate Theory (CLPT) to predict the elastic properties of epoxy laminates reinforced with Pineapple Leaf Fiber (PALF) and Grewia Optiva. Based on systematic variation in fiber content and stacking architecture, the following conclusions are drawn:

- The CLPT-based model effectively predicted longitudinal modulus ( $E_{xx}$ ), transverse modulus ( $E_{yy}$ ), shear modulus ( $G_{xy}$ ), and Poisson's ratio ( $\mu_{xy}$ ), offering a reliable alternative to finite element modeling.
- Increasing PALF content from 10 wt.% to 20 wt.% consistently enhanced laminate stiffness, confirming PALF's dominant role in axial and shear performance.
- The  $A_3$  stacking sequence ( $[0/45/90/30]$ ) exhibited the highest longitudinal modulus (37.32 GPa at 20 wt.% PALF), demonstrating its suitability for load-bearing applications.
- The  $A_1$  laminate ( $[0/\pm 45/90]$ ) provided superior shear modulus across all fiber compositions, highlighting its balanced layup efficiency.
- The  $A_2$  configuration ( $[0/(45)_2/-30]$ ) showed the maximum Poisson's ratio (0.310 at 20 wt.% PALF), but comparatively lower stiffness, indicating greater transverse compliance.
- Clear correlations emerged between stacking sequence and mechanical response:  $A_3$  optimized longitudinal and transverse stiffness,  $A_1$  maximized shear modulus, while  $A_2$  favored compliance.
- The quasi-mathematical approach significantly reduced computational intensity compared to FEM, enabling faster preliminary laminate design evaluations.
- Model predictions aligned with previously reported experimental and computational studies, reinforcing the validity of the methodology.
- The hybridization of PALF with Grewia Optiva demonstrated a promising pathway for lightweight, eco-friendly laminates with balanced mechanical properties.
- These findings establish a foundation for designing sustainable composite laminates for automotive and structural engineering applications.

This study confirms that combining underutilized natural fibers with optimized stacking architecture can deliver tailored stiffness–compliance performance. The computational framework presented here provides a scalable tool for sustainable composite design, bridging the gap between experimental trials and industrial application.

Future work should focus on experimental validation of the model predictions, inclusion of environmental factors such as moisture and thermal effects, and extension to dynamic loading scenarios. Integration of machine learning with quasi-mathematical modeling could further enhance predictive accuracy and accelerate the development of next-generation bio-composites.

### **Acknowledgment**

We acknowledge UPES Dehradun for providing the research lab facilities for experimentation.

### **Authors' Contribution**

"Mayank Bhardwaj: Conceptualization, Data curation, Investigation, Visualization, Writing, original draft, software; Jitendra Yadav: Project administration, Supervision, Methodology, Writing review and editing, and Brijesh Gangil: Supervision, Formal analysis, Project administration, Funding acquisition, Writing, review and editing."

### **Conflict of Interest**

The authors of this work state that they have no conflicts of interest about its publication.

### **Ethics Approval**

No ethical clearance certificate is applicable for present study. The authors of the submitted paper did not receive support from any organization.

### **Funding**

No specific grant from a public, private, or nonprofit organization was obtained for this study.

### **References**

1. F. Ozturk, M. Cobanoglu, and R. E. Ece (2024), Journal of Thermoplastic Composite Materials, Recent advancements in thermoplastic composite materials in aerospace industry, vol. 37, no. 9, pp. 3084–3116.
2. P. Rath, M. Jindal, and T. Jindal (2021) A review on economically-feasible and environmental-friendly technologies promising a sustainable environment, Clean Eng Technol, vol. 5, p. 100318
3. A. Dhandapani et al.(2024), Evolution, Prospects, and Predicaments of Polymers in Marine Applications: A Potential Successor to Traditional Materials, Recycling 2024, Vol. 9, Page 8, vol. 9, no. 1, p. 8

4. Z. H. Boon, Y. Y. Teo, and D. T. C. Ang, (2022) Recent development of biodegradable synthetic rubbers and bio-based rubbers using sustainable materials from biological sources, *RSC Adv*, vol. 12, no. 52, pp. 34028–34052
5. C. Andreeßen and A. Steinbüchel (2018) “Recent developments in non-biodegradable biopolymers: Precursors, production processes, and future perspectives,” *Applied Microbiology and Biotechnology* 2018 103:1, vol. 103, no. 1, pp. 143–157
6. A. P. C. Faaij (2022) Repairing What Policy Is Missing Out on: A Constructive View on Prospects and Preconditions for Sustainable Biobased Economy Options to Mitigate and Adapt to Climate Change, *Energies* 2022, Vol. 15, Page 5955, vol. 15, no. 16, p. 5955
7. A. Ali and J. D. Russell, (2025) Accelerating the Transition to Wood-Based Circular Bioeconomy: A Literature Review of Current State, Trends, Opportunities, and Priorities for Future Research, *Current Forestry Reports* 2025 11:1, vol. 11, no. 1, pp. 1–20
8. V. Prasad, A. Alliyankal Vijayakumar, T. Jose, and S. C. George (2024) A Comprehensive Review of Sustainability in Natural-Fiber-Reinforced Polymers, *Sustainability* 2024, Vol. 16, Page 1223, vol. 16, no. 3, p. 1223
9. S. H. Kamarudin et al. (2022) A Review on Natural Fiber Reinforced Polymer Composites (NFRPC) for Sustainable Industrial Applications, *Polymers* 2022, Vol. 14, Page 3698, vol. 14, no. 17, p. 3698
10. S. Palanisamy, K. Vijayananth, T. M. Murugesan, M. Palaniappan, and C. Santulli (2024) The prospects of natural fiber composites: A brief review, *International Journal of Lightweight Materials and Manufacture*, vol. 7, no. 4, pp. 496–506
11. S. J. Skosana, C. Khoathane, and T. Malwela (2025) Driving towards sustainability: A review of natural fiber reinforced polymer composites for eco-friendly automotive light-weighting, *Journal of Thermoplastic Composite Materials*, vol. 38, no. 2, pp. 754–780
12. O. Akampumuza, P. M. Wambua, A. Ahmed, W. Li, and X. H. Qin (2017) Review of the applications of biocomposites in the automotive industry, *Polym Compos*, vol. 38, no. 11, pp. 2553–2569

13. S. Sharma, P. Sudhakara, S. K. Misra, and J. Singh (2020) A comprehensive review of current developments on the waste-reinforced polymer-matrix composites for automotive, sports goods and construction applications: Materials, processes and properties, *Mater Today Proc*, vol. 33, pp. 1671–1679
14. A. Fitzgerald et al.(2021) A Life Cycle Engineering Perspective on Biocomposites as a Solution for a Sustainable Recovery, *Sustainability* 2021, Vol. 13, Page 1160, vol. 13, no. 3, p. 1160
15. V. C. Martins, S. Cutajar, C. V. van der Hoven, P. Baszyński, and H. Dahy,(2020) FlexFlax Stool: Validation of Moldless Fabrication of Complex Spatial Forms of Natural Fiber-Reinforced Polymer (NFRP) Structures through an Integrative Approach of Tailored Fiber Placement and Coreless Filament Winding Techniques, *Applied Sciences* 2020, Vol. 10, Page 3278, vol. 10, no. 9, p. 3278
16. M. R. M. Asyraf et al.(2022) Product Development of Natural Fibre-Composites for Various Applications: Design for Sustainability, *Polymers* 2022, Vol. 14, Page 920, vol. 14, no. 5, p. 920,
17. J. Neto et al.(2022) A Review of Recent Advances in Hybrid Natural Fiber Reinforced Polymer Composites, vol. 13, no. 20, p. 3511
18. M. J. Suriani et al.(2021) Critical Review of Natural Fiber Reinforced Hybrid Composites: Processing, Properties, Applications and Cost, *Polymers* 2021, Vol. 13, Page 3514, vol. 13, no. 20, p. 3514
19. J. Neto et al (2023), A Review of Recent Advances in Hybrid Natural Fiber Reinforced Polymer Composites,.
20. G. Jogur, A. Nawaz Khan, A. Das, P. Mahajan, and R. Alagirusamy (2018) Impact properties of thermoplastic composites, *Textile Progress*, vol. 50, no. 3, pp. 109–183
21. S. Sakib et al(2023) Effect of fibre orientation and stacking sequence on properties of hybrid composites, *Materials Science and Technology (United Kingdom)*, vol. 39, no. 13, pp. 1627–1639
22. [22] A. Husain, S. H. Khan, and A. H. I. Mourad (2025) Stacking sequence effects on flexural stiffness, failure progression, and energy absorption in asymmetric CFRP laminates, *Results in Engineering*, vol. 27, p. 105863

23. T. Islam et al.(2024) Advancements and challenges in natural fiber-reinforced hybrid composites: A comprehensive review, *SPE Polymers*, vol. 5, no. 4, pp. 481–506
24. L. F. Ng et al(2023), State-of-the-art review on developing lightweight fiber-metal laminates based on synthetic/natural fibers, *Polym Compos*, vol. 44, no. 10, pp. 6275–6303
25. S. K. Selvaraj and K. Saravanan (2024) Characterization and potential applications of *Grewia hirsuta* fibers: nature's own composite materials, *Biomass Conversion and Biorefinery* 2024 15:4, vol. 15, no. 4, pp. 5769–5777
26. T. Raja, Y. Devarajan, and S. Vickram (2025) Evaluation of *Grewia optiva* fiber as a sustainable and high-performance reinforcement material for composite applications, *Results in Engineering*, vol. 25, p. 104096
27. F. E. Bock, R. C. Aydin, C. J. Cyron, N. Huber, S. R. Kalidindi, and B. Klusemann (2019) A review of the application of machine learning and data mining approaches in continuum materials mechanics, *Front Mater*, vol. 6, p. 452701
28. X. Li (2025) Multiscale computational modeling of 3D printed continuous Fiber reinforced polymer composites, *Scientific Reports* 2025 15:1, vol. 15, no. 1, pp. 1–18
29. C. R. Picu (2021) Constitutive models for random fiber network materials: A review of current status and challenges, *Mech Res Commun*, vol. 114, p. 103605
30. M. Venkateswar Reddy, B. Hemasunder, S. V. Ramana, P. Ramesh Babu, P. Thejasree, and J. Joseph (2023), State of art on FEM approach in inverse heat transfer problems for different materials, *Mater Today Proc*, Jul. 2023,
31. A. Haider (2024) Efficiency enhancement techniques in finite element analysis: navigating complexity for agile design exploration, *Aircraft Engineering and Aerospace Technology*, vol. 96, no. 5, pp. 662–668,
32. P. P. Bijlwan, L. Prasad, and A. Sharma (2024) Analysis of mechanical properties and free vibrational characteristics of novel *Grewia optiva*/basalt fiber reinforced hybrid polymer composites, *J Appl Polym Sci*, vol. 141, no. 13, p. e55165
33. K. Kalauni and S. J. Pawar,(2023) “Physicochemical, mechanical, morphological, and thermal characterization of *Grewia Optiva* fiber reinforced epoxy and hybrid (epoxy-Lannea Coromandelica gum) resins composite, *Journal of Polymer Research* 2023 30:6, vol. 30, no. 6, pp. 1–19

34. R. Bu, Y. Xiong, and C. Zhang, (202)  $\pi$ - $\pi$  Stacking Contributing to the Low or Reduced Impact Sensitivity of Energetic Materials, *Cryst Growth Des*, vol. 20, no. 5, pp. 2824–2841
35. B. Geng, P. Deng, Y. Li, and J. Hu (2023). Experimental and first-principles calculation study on influence of stacking faults on hardness and anisotropy of  $M_7C_3$  carbides," *J Alloys Compd*, vol. 968, p. 172276
36. D. Nath, Ankit, D. R. Neog, and S. S. Gautam (2024). *Archives of Computational Methods in Engineering*, vol. 31, no. 5. Application of Machine Learning and Deep Learning in Finite Element Analysis: A Comprehensive Review. pp. 2945–2984
37. J. Kudela and R. Matousek (2022). *Soft Computing*. Recent advances and applications of surrogate models for finite element method computations: a review," 2022 26:24, vol. 26, no. 24, pp. 13709–13733
38. G. S. Bhadane and S. B. Patil (2023) *Mater Today Proc*, vol. 72. Mathematical modeling of multilayered composite material to obtain in plane elastic constants, pp. 794–801,